Catalysis Today 317 (2018) 12–20

Contents lists available at ScienceDirect

Catalysis Today

journal homepage: www.elsevier.com/locate/cattod

Preparation of a highly active ternary Cu-Zn-Al oxide methanol synthesis catalyst by supercritical CO_2 anti-solvent precipitation

Simon A. Kondrat[a,b], Paul J. Smith[a], Li Lu[c], Jonathan K. Bartley[a], Stuart H. Taylor[a], Michael S. Spencer[a], Gordon J. Kelly[d], Colin W. Park[d], Christopher J. Kiely[a,c], Graham J. Hutchings[a,*]

[a] Cardiff Catalysis Institute, School of Chemistry, Cardiff University, Main Building, Park Place, Cardiff, CF10 3AT, UK
[b] Department of Chemistry, Loughborough University, Loughborough, Leicestershire, LE11 3TU, UK
[c] Department of Materials Science and Engineering, Lehigh University, 5 East Packer Avenue, Bethlehem, PA, 18015-3195, USA
[d] Johnson Matthey, P.O. Box 1, Belasis Avenue, Cleveland, TS23 1LB, UK

ARTICLE INFO

Keywords:
Georgeite
Methanol synthesis
Copper zinc oxide
Alumina addition

ABSTRACT

Methanol synthesis using $Cu/ZnO/Al_2O_3$ catalysts is a well-established industrial process. Catalyst development is always an important factor and this has resulted in the current fully optimised commercial catalyst that is prepared by co-precipitation *via* hydroxycarbonate precursors. Recently, the synthesis of a CuZn hydroxycarbonate precursor, analogous to the rare mineral georgeite, was reported to produce a high activity methanol synthesis catalyst. Here we report the addition of Al^{3+}, the third component found in industrial catalysts, to the zincian georgeite-derived catalyst prepared using a supercritical CO_2 anti-solvent precipitation methodology. The co-addition of an AlO(OH) sol to the Cu/Zn precursor solution was found to not disrupt the formation of the CuZn georgeite phase, while providing efficient mixing of the Al^{3+} within the material. The catalyst derived from the CuZn georgeite precursor phase doped with Al^{3+} showed a high level of methanol synthesis productivity, which was comparable to that of the binary CuZn georgeite derived catalyst. This material also exhibited enhanced stability during an accelerated ageing test compared to the non-Al doped zincian georgeite material. Performance was benchmarked against an industrially relevant $Cu/ZnO/Al_2O_3$ standard catalyst.

1. Introduction

$Cu/ZnO/Al_2O_3$ is a well-studied commercial catalyst used in the synthesis of methanol from syn-gas (CO, CO_2 and H_2) and in the low-temperature water-gas shift reaction (LTS) [1,2]. Both reactions are industrially important, with methanol being an important chemical intermediate having a worldwide demand exceeding 50 M tons per annum and the LTS reaction being used up-stream of many industrial processes for H_2 production and CO removal [2]. In addition, both reactions have contemporary applications in green chemistry, namely: (i) for methanol synthesis using captured CO_2 and renewably sourced H_2 [3,4] and (ii) LTS reaction is used to remove trace amounts of CO from fuel cell gas streams where it can act as a poison [5].

The active site of the $Cu/ZnO/Al_2O_3$ catalyst has long been considered be associated with metallic Cu [6], although the role of ZnO in both methanol synthesis and LTS has been intensely debated. ZnO can act as a dispersant for Cu, a hydrogen reservoir and a poison scavenger. It could also have a direct role in the reaction mechanism through activation of CO_2 or through generation of an active site resulting from a Cu-Zn interaction [7–12]. A range of in-depth characterisation studies have demonstrated a strong metal support interaction between Cu and ZnO, with partial ZnO reduction at the interface with Cu under near operating conditions [8,13,14]. Consequently, two structures for the active site are typically considered; namely a Cu-Zn surface alloy or an interfacial synergy between Cu/ZnO. While this Cu-Zn interaction has formed the focus of many structure/ activity studies, the third component of the industrial catalyst, namely Al_2O_3 (and Al^{3+} in particular) is often overlooked.

The addition of Al^{3+} and, occasionally, Ga^{3+} into the Cu-Zn oxide binary system has long been known, from a practical perspective, to enhance catalyst stability [15–17]. The loading of Al_2O_3 within industrial catalysts varies between 10 wt.% and 20 wt.%, with higher loadings being used in LTS catalysts than for methanol synthesis catalysts, due to the more aggressive conditions encountered in the LTS

* Corresponding author.
E-mail address: hutch@cardiff.ac.uk (G.J. Hutchings).

https://doi.org/10.1016/j.cattod.2018.03.046
Received 17 October 2017; Received in revised form 22 March 2018; Accepted 23 March 2018
Available online 26 March 2018

reaction [17]. Taking these loadings into account, it is clear that Al_2O_3 does not act as a conventional support material. Typically the Al_2O_3 additive has been thought of as a binder to retain the structural integrity of catalyst pellets under operational conditions [16]. Recently, Behrens et al. have shown that Al^{3+} serves as a catalytic promoter by acting as a substitutional n-type semiconductor dopant in ZnO, which modifies the defect chemistry and reducibility of the ZnO support [15].

Achieving high Cu surface area, a strong metal-support interaction between Cu and ZnO and the efficient incorporation of promoters is highly dependent on the exact method of catalyst preparation. Specific copper-zinc hydroxycarbonate phases, such as zincian malachite, have been found to be suitable catalyst precursors; providing a high degree of mixing between components and morphologies that result in a high Cu surface area [18–20]. Recently, we demonstrated that a supercritical CO_2 anti-solvent (SAS) preparation method [21] can be used to prepare an often-neglected hydroxycarbonate material, analogous to the rare amorphous mineral georgeite [22], which on calination and reduction produces highly dispersed Cu in a poorly crystalline ZnO matrix [23]. The catalyst derived from this zincian georgeite precursor material showed excellent initial methanol synthesis activity, but displayed inferior stability compared to more conventional Al^{3+} containing catalysts. Given the nature of the SAS preparation technique, adding a third component to the catalyst precursor system is not trivial task. Here, we report the successful addition of ~20 at.% Al^{3+} into Cu/ZnO catalysts prepared by the SAS technique and investigate the effect of this promoter on the catalytic activity and stability.

2. Experimental

2.1. Supercritical antisolvent (SAS) precipitation

SAS precipitated materials were prepared as follows; 4 mg ml^{-1} copper(II) acetate monohydrate (Sigma Aldrich, > 99.0% purity) and 2.13 mg ml^{-1} zinc(II) acetate dihydrate (Sigma Aldrich, > 99.0% purity) were dissolved in ethanol (Fischer Scientific, absolute > 99.8%) containing 10 vol% water to give a nominal Cu:Zn molar ratio of 2:1. Two different Al^{3+} complexes were investigated to prepare ternary Cu:Zn:Al oxyhydroxide samples, with a ratio of 5/3/2 respectively. One complex, aluminium(III) lactate (Sigma Aldrich 95.0% purity) was dissolved in the Cu/Zn ethanol-water solution prior to SAS precipitation. The alternative Al^{3+} source was to use a sol of aluminium boehmite (AlO(OH)) (Johnson Matthey-stabilised with dilute nitric acid) mixed with the Cu/Zn ethanol-water solution. In the ternary salt solutions 3.56 mg ml^{-1} copper acetate, 1.96 mg ml^{-1} zinc acetate and 0.232 mg ml^{-1} aluminium boehmite or 0.87 mg ml^{-1} aluminium lactate were used. Samples will be referred to as Cu/Zn/Al-$C_3H_5O_3$ when using the lactate derived precursor, Cu/Zn/Al- AlO(OH) with the boehmite precursor, Cu/Zn for the binary zincian georgeite and Cu/Zn/Al-Std for industrial standards.

SAS precipitation experiments were performed using an apparatus manufactured by Separex. Liquefied CO_2 was pumped at a flow rate of 6.5 kg h^{-1} and the whole system was pressurised to 110 bar and held at 40 °C to form supercritical carbon dioxide ($scCO_2$). Initially pure solvent was pumped, concurrently with $scCO_2$, through the fine capillary into the precipitation vessel, with a flow rate of 6.5 ml min^{-1} for 15 min to obtain steady state conditions. The Cu/Zn or Cu/Zn/Al precursor solutions were then delivered at a flow rate of 6.5 ml min^{-1}, giving an $scCO_2$:metal solution molar ratio of 22:1. Following the delivery of the metal salt solutions, pure ethanol was pumped at 6.5 ml min^{-1} concurrently with $scCO_2$ for 30 min, before finally flowing only $scCO_2$ over the sample for a further 1 h. The vessel was then depressurised to atmospheric pressure and the precipitate collected. Experiments were conducted for approximately 3.5 h, which resulted in the synthesis of approximately 1.1–1.5 g of solid. Recovered samples were then calcined at 300 °C for 4 h in static air (ramp rate 1 °C min^{-1}).

2.2. Catalyst characterisation

X-ray diffraction (XRD) of precursors and catalysts was performed on a (θ-θ) PANalytical X'pert Pro powder diffractometer equipped with a Ni filtered CuK_α radiation source operating at 40 keV and 40 mA. Diffraction patterns were recorded over a 10–80° 2θ angular range using a step size of 0.016°. Crystallite sizes were determined using the Scherrer equation.

Infrared spectroscopy was performed on the SAS catalyst precursors using a Bruker Vertex 70 IR spectrometer equipped with a single reflection diamond attenuated total reflectance accessory and a mercury cadmium telluride (MCT) detector.

Brunauer Emmett Teller (BET) surface area analysis was performed using a Micromeritics Gemini 2360 surface analyser. Five-point isotherms were obtained using N_2 at −196.15 °C with surface area analysis carried out using a BET plot in the P/P_0 range 0.06–0.35. Cu surface area analysis was carried out on a Quantachrome ChemBET chemisorption analyser equipped with a thermal-conductivity detector (TCD). Calcined samples (100 mg) were reduced to generate active catalysts using a 10% H_2/Ar mixture (30 ml min^{-1}) by heating to 140 °C at 10 °C min^{-1}, and then to 225 °C at 1 °C/min. The resulting catalysts were cooled to 65 °C under He for N_2O pulsing. Twelve N_2O pulses (113 µl each) were followed with three N_2 pulses for calibration purposes. The amount of N_2 emitted was assumed to be equivalent to half a monolayer coverage of oxygen and the surface density of Cu was calculated to be 1.47×10^{19} atoms m^{-2}. To account for the significant mass loss on reduction for Cu surface area analysis, the difference in sample mass (with quartz reactor) before and after testing was used to determine a percentage mass loss. Cu surface areas are quoted as m^2 per g of reduced catalyst.

Thermal gravimetric analysis (TGA) and differential thermal analysis (DTA) were performed using a Setaram Labsys 1600 instrument. Samples (20–50 mg) were loaded into alumina crucibles and heated to 600 °C (5 °C min^{-1}) in a flow of synthetic air (50 ml min^{-1}).

Elemental analysis was performed using Energy-dispersive X-ray (XEDS) analysis in an SEM. The specimens were dispersed onto adhesive carbon tape, mounted on 12.5 mm aluminium sample stubs. Analysis was performed using a Zeiss Evo 40 scanning electron microscope with an Oxford Instruments Model 7636 LN2 cooled SiLi XEDS detector, operated at 25 kV and 1000 pA.

Samples for scanning transmission electron microscopy (STEM) were prepared by drop casting of a diluted aqueous sol onto a carbon coated molybdenum mesh TEM grid (Electron Microscopy Sciences). The samples were analysed in an aberration corrected JEOL ARM 200CF analytical electron microscope equipped with a JEOL Centurio XEDS system operating at 200 kV. Images were collected in high angle annular dark field (HAADF) and high resolution (HR) STEM mode. Fast Fourier Transforms (FFTs) derived from the HAADF-TEM images were used to measure interplanar spacing and angles.

2.3. Catalyst testing

Methanol synthesis testing was performed in a six-tube parallel fixed bed flow reactor system with an additional by-pass line. The reactor was charged with unreduced catalyst (0.5 g). Samples were then reduced *in-situ* by heating to 225 °C at 1 °C min^{-1} using a 2% H_2/N_2 gas mixture (60 ml min^{-1}). Catalysts were then exposed to the synthetic syngas (CO : CO_2 : H_2 : N_2 composition = 6 : 9.2 : 67 : 17.8 *mol.* %) at 3.5 L h^{-1}, 25 bar pressure and temperatures between 190 and 250 °C. A mass hourly space velocity of 7200 L kg^{-1} h^{-1} was used throughout the reaction. LTS testing was performed in a similar parallel fixed bed reactor with a single stream feed and an additional by-pass line. As with methanol synthesis, the catalysts (0.5 g) were reduced *in-situ*, in an identical manner to that described above. Catalysts were subjected to synthetic syngas and vaporised water (H_2O : CO : CO_2 : H_2 : N_2 = 50 : 2 : 8 : 27.5 : 12.5 mol. %.) at 27.5 bar pressure and a temperature of

220 °C. A mass hourly space velocity of 75,000 L kg^{-1} h^{-1} was used throughout the reaction. For both reactions, in-line FT-IR analysis was used to detect CO, CO_2, H_2O and CH_3OH. Higher alcohols and other liquids were trapped downstream and quantified by GC analysis offline. Catalyst productivities and activities were determined from the mass of Cu within the reactor, considering the mass loss of samples on reduction (determined during copper surface area analysis) and the Cu content as determined from elemental analysis.

3. Results and discussion

The preparation of binary Cu/Zn and ternary Cu/Zn/Al georgeite derived catalysts was, as stated in the introduction, performed using the SAS precipitation methodology. As with precipitation methodologies the choice of metal precursor salt has a significant effect on the product produced. The key factor in choice of metal precursor is that the salt is soluble in the precursor solvent, in this case a water-ethanol mixture, but insoluble in the supercritical carbon dioxide anti-solvent. Frequently metal acetate salts are chosen [21], although it was found that aluminium triacetate was unsuitable due it its relatively high solubility in supercritical carbon dioxide. Therefore, aluminium lactate, fulfilled the desired criterion. It is acknowledged that a range of other potential aluminium complexes could be potentially used in the SAS process.

An additional strategy would be to precipitate the binary Cu/Zn system in the presence of a preformed metal oxide or hydroxide. Previously we have shown this to be successful in a batch process for the deposition of Co onto pre-formed TiO_2 [24]. An issue with performing this in the continuous SAS process is the formation of blockages in the co-axial nozzle used for delivery of metal salt solutions. Therefore, a suspension of colloidal AlO(OH) was used as an alternative solid aluminium source.

The composition of the SAS precipitates prepared by the lactate and AlO(OH) routes was investigated to determine how much of the third Al^{3+} component was incorporated into the final product compared to the nominal Cu:Zn target ratio of 2:1. The results shown in Table 1 demonstrates that all three metal components were contained in the SAS precipitate, although the exact target ratios were not achieved. The target Cu:Zn ratio of 2:1 was attained in Cu/Zn/Al- AlO(OH), while a slight Cu deficiency was noted in Cu/Zn/Al-$C_3H_5O_3$. This small deficiency in Cu was considered tolerable for the purposes of this initial study. The small deviations from the nominal Cu:Zn:Al target ratios demonstrate the complexity of controllably adding a third precursor component to the SAS precipitation. However, the compositions experimentally obtained are deemed to be sufficiently close to allowing us to ascertain the viability of the process and discern the need for further refinement later.

Table 1
Physical characteristics of the various SAS precipitates produced and their associated catalysts after calcination and reduction treatment.

Sample	Cu:Zn:Al Molar Ratio[a,b]	Surface area of SAS precipitate (m^2 g^{-1})[c]	Surface area of calcined sample (m^2 g^{-1})[c]	Cu surface area in reduced catalysts (m^2 g_{Cu}^{-1})[d]
Cu/Zn	2:1	97	85	47
Cu/Zn/Al-$C_3H_5O_3$	5.7:2.5:1.8	114	30	18
Cu/Zn/AlO(OH)	5.1:2.5:2.4	92	90	54
Cu/ZnO/Al_2O_3-standard material	5/3/2	–	–	44

[a] Composition determined by XEDS analysis (error ± 3%).
[b] Target composition 2/1 or 5/3/2.
[c] Surface areas determined by BET analysis.
[d] Surface area determined from N_2O titration after reduction at 225 °C.

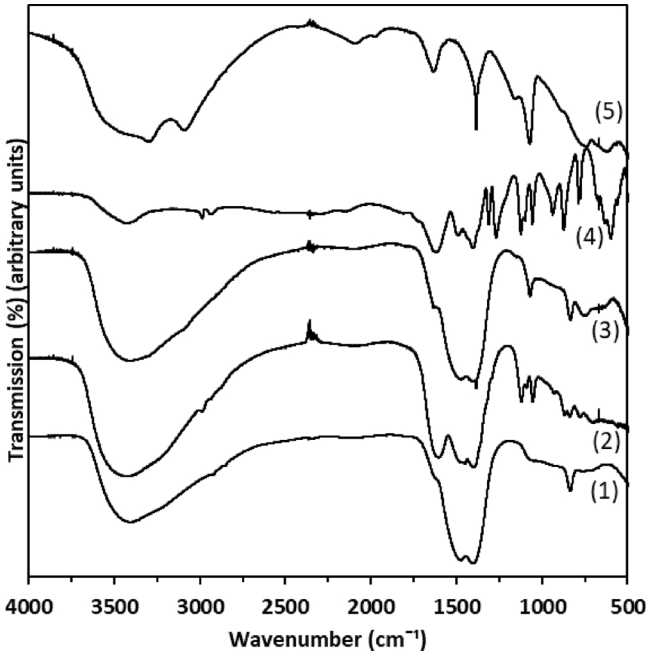

Fig. 1. FT-IR spectra of SAS prepared zincian georgeite precursors with and without Al^{3+} precursors. (1) Binary zincian georgeite, (2) Cu/Zn/Al-$C_3H_5O_3$ (3) Cu/Zn/AlO(OH) (4) aluminium lactate only and (5) aluminium boehmite only.

IR spectroscopy was then used to ascertain the nature of both SAS precipitated Cu/Zn/Al precursor materials, relative to that of the SAS prepared zincian georgeite material reported previously (Fig. 1). In regard to binary CuZn hydoxycarbonates IR spectra are well reported and can be used to identify the phase present in the methanol synthesis catalyst precursor [25]. Indeed, the mineral georgeite is classified based on it IR spectrum, given that it is amorphous and so cannot identified by XRD [22]. Both of the Al^{3+} containing SAS samples had bands characteristic of zincian georgeite [22] (the 3419 cm^{-1} peak corresponds to ν(O—H), while those at 1475 and 1408 cm^{-1} can be assigned to $\nu_3(CO_3^{2-})$, 1049 cm^{-1} to $\nu_1(CO_3^{2-})$ and 836 cm^{-1} to $\nu_2(CO_3^{2-})$), indicating that this basis phase is retained. Additional bands, to those found in zincian georgeite, were also observed for both Al-containing samples and could be assigned to bands originating from aluminium lactate and AlO(OH). The retention of the Al^{3+} precursor ligands on SAS precipitation clearly differs from that of the copper and zinc acetate salts, which undergo an exchange of ligand for carbonate and hydroxide, attributable to the formation of carbonic acid in the CO_2-H_2O-C_2H_5OH phase system.

Powder X-ray diffraction of the catalyst precursors (Fig. 2) showed no strong reflections associated with known Cu/Zn hydroxycarbonates, such as malachite or aurichalcite [25]. As zincian georgeite is highly amorphous [22,23,26,27] we conclude, in conjunction with the observed IR bands, that this is the predominant phase in all samples. A weak diffraction pattern for AlO(OH) was seen in the Cu/Zn/Al- AlO(OH) sample, reinforcing the conclusion from IR data that aluminium boehmite is retained on precipitation. Interestingly, no diffraction peaks associated with aluminium lactate were detected in contrast to the strong diffraction pattern of the unprocessed aluminium(III) lactate. The loss of long-range order with SAS precipitation is often observed and is due to the very rapid nucleation rates afforded by the process [21].

In addition to retention of the amorphous zincian georgeite type phase, it is important that the ternary Cu/Zn/Al catalyst precursors have a high surface area to ensure a high dispersion of Cu in the calcined and activated catalyst. Surface area analysis (Table 1)

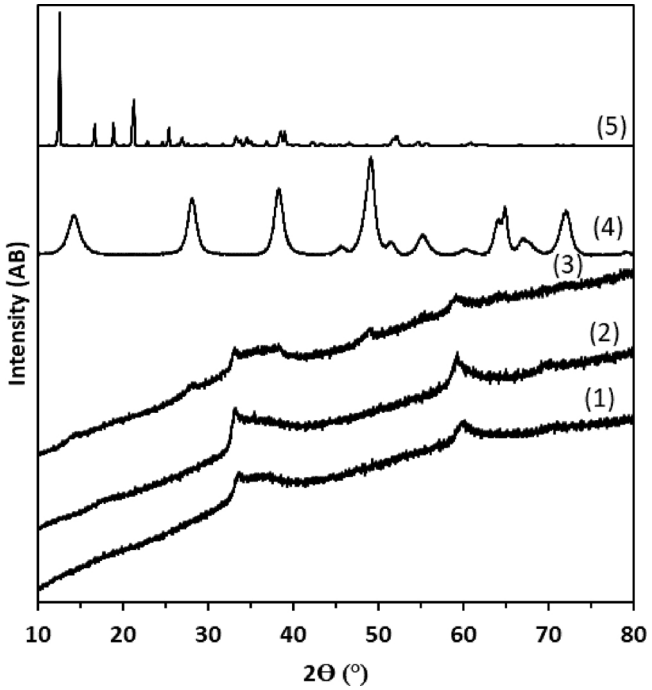

Fig. 2. XRD patterns of SAS prepared zincian georgeite precursors with various Al^{3+} precursors: (1) binary zincian georgeite, (2) Cu/Zn/Al-$C_3H_5O_3$ (3) Cu/Zn/AlO(OH) (4) aluminium boehmite only and (5) aluminium lactate only.

demonstrates that the both Cu/Zn/Al-$C_3H_5O_3$ and Cu/Zn/Al-AlO(OH) had comparable surface areas to the binary zincian georgeite material. While all the samples had reasonable surface areas prior to calcination, its retention during the catalyst activation stage is highly dependent on the correct choice of heat treatment temperature, which can be determined from TGA/DTA testing.

Previous TGA studies of the binary-zincian georgeite phase showed that the material had a highly distinctive three-stage thermal decomposition profile, in contrast to the single stage decomposition displayed by many other conventional crystalline hydroxycarbonate catalyst precursors [23]. TGA coupled with DTA was performed on the two Al containing precursor materials and contrasted with that of the binary zincian georgeite catalyst precursor (Fig. 3). An important mass loss step is the final one centred at *ca.* 450 °C for the binary zincian georgeite material, which has previously been shown to be exclusively due to carbonate decomposition and is often referred to in the literature to as “high temperature carbonate”. The decomposition temperature of this carbonate component is a good descriptor for the extent of CuO-ZnO mixing, with high temperature being associated with greater interaction between CuO and ZnO [28]. In turn, the degree CuO-ZnO mixing influences the Cu surface area andCu-ZnO interaction in the final activated catalyst and therefore to an extent is an effective indicator of catalytic activity. The addition of Al into the zincian georgeite precipitate *via* the aluminium boehmite precursor resulted in a slight reduction in the high temperature carbonate decomposition from 450 °C to *ca.* 430 °C. It is expected that Al^{3+} incorporation would stabilise the disordered ZnO produced from SAS precipitation and so increase the decomposition temperature of high temperature carbonate. The opposite observation indicates a partial disruption in the Cu-Zn mixing within the zincian georgeite phase, potentially due to the AlO(OH) sol disrupting the phase system during SAS precipitation, which results in a more phase separated CuO and ZnO. Further it would indicate little incorporation of Al^{3+} into the zincian georgiete. The change in the high temperature carbonate decomposition peak (relative to the binary zincian georgeite) was far greater for Cu/Zn/Al-$C_3H_5O_3$ than Cu/Zn/Al-AlO(OH). A significantly greater mass loss occurred during the second step (centred at *ca.* 200 °C) which resulted in a smaller third mass loss, which happened at a far lower temperature than that for the pure zincian georgeite (*ca.* 290 °C as compared to 450 °C). While the initial Cu/Zn/Al oxyhydroxide precipitate derived from the L-lactate precursor may be well mixed and exhibits a suitable surface area, the significant exothermic reaction during decomposition (as observed from DTA data - Fig. 3b) results in a severe modification of the materials nanostructure and Cu-Zn interaction. A similar effect has previously been observed when calcining the copper and zinc acetate complexes that are retained after SAS precipitation, due to the lack of water co-solvent [29]. The implication from the TGA/DTA results is that the Cu/Zn/Al oxyhydroxide sample prepared with the Cu/Zn/Al-$C_3H_5O_3$ precursor would give a poor Cu surface area and therefore inferior activity upon subsequent calcination and reduction during the activation process.

Given previous reports that the retention of high temperature carbonate after calcination can be beneficial to performance, it was considered that 300 °C would be a suitable calcination temperature. The required characteristics of the calcined materials are (i) high surface area, (ii) poor crystallinity and (iii) well-mixed CuO-ZnO with Al_2O_3 (in the ternary catalysts). The surface areas of the calcined materials are presented in Table 1. While the addition of AlO(OH) had no negative effect on final surface area (with a value of 90 $m^2 g^{-1}$ compared to 85 $m^2 g^{-1}$ for the corresponding zincian georgeite material) the exothermic decomposition of Cu/Zn/Al-$C_3H_5O_3$ reduced the surface area to 30 $m^2 g^{-1}$.

Evaluation of the powder X-ray diffraction data from the calcined materials (Fig. 4) shows that calcined Cu/Zn/Al-$C_3H_5O_3$ materials was more crystalline compared to the calcined Cu/Zn/AlO(OH), as a more intense diffraction pattern (both in terms of peak height and area) associated with CuO was observed in the former. Both Al containing samples can be described as more crystalline than the more the reference zincian georgeite, which had no characteristic CuO reflections from XRD. It should be noted that calcined zincian georgeite is not amorphous in nature but comprises of nanocrystalline CuO and ZnO below the detection limit of XRD [23]. It is likely that the reduced area of the CuO reflections seen in calcined Cu/Zn/AlO(OH), relative to Cu/Zn/Al-$C_3H_5O_3$ which has the same Cu mass content (shown in Table 1), is due to the presence of a significant contribution of sub 3 nm crystallites that are undetectable by XRD. Larger crystallites can be detected from XRD (6 nm) indicating a distribution of particle sizes above and below the XRD detection limit. The stronger reflections associated with calcined Cu/Zn/Al-$C_3H_5O_3$ were calculated to have a mean average size of 7 nm, with fewer undetected nanocrystallites present. The observed trend in CuO crystallite size correlates well with the position of the high temperature carbonate decomposition peak from TGA analysis and the reported surface areas. Another point worth noting from XRD analysis of the Cu/Zn/Al catalyst derived from aluminium boehmite precursor was that the AlO(OH) phase was retained and no crystalline Al_2O_3 phase was detected. Asa higher temperature calcination treatment would be required to convert the AlO(OH) to Al_2O_3which would inevitably be detrimental to the CuO crystallite size and final Cu surface area in the reduced catalyst, it was decided that further analysis and testing would be performed on the 300 °C calcined material containing the AlO(OH) phase. Also of note is the absence of crystalline Al_2O_3 in the calcined Cu/Zn/Al-$C_3H_5O_3$, which suggests that either nanocrystalline Al_2O_3 or alternative Al compound is present.

A clear trend emerging from the combined XRD, BET and TGA data was that the choice of the Al^{3+} precursor has a significant effect on the catalyst properties. A further point to consider is that the characterisation work presented so far has been of the calcined CuO/ZnO/ Al phase material and not the final reduced Cu/ZnO catalyst that is exposed to the reaction mixtures. A well-known method for probing the Cu surface area is by N_2O chemisorption of a pre-reduced catalyst sample. While the technique potentially also measures reduced Zn/ZnO_x content at the interface with the reduced Cu particles [30] it is

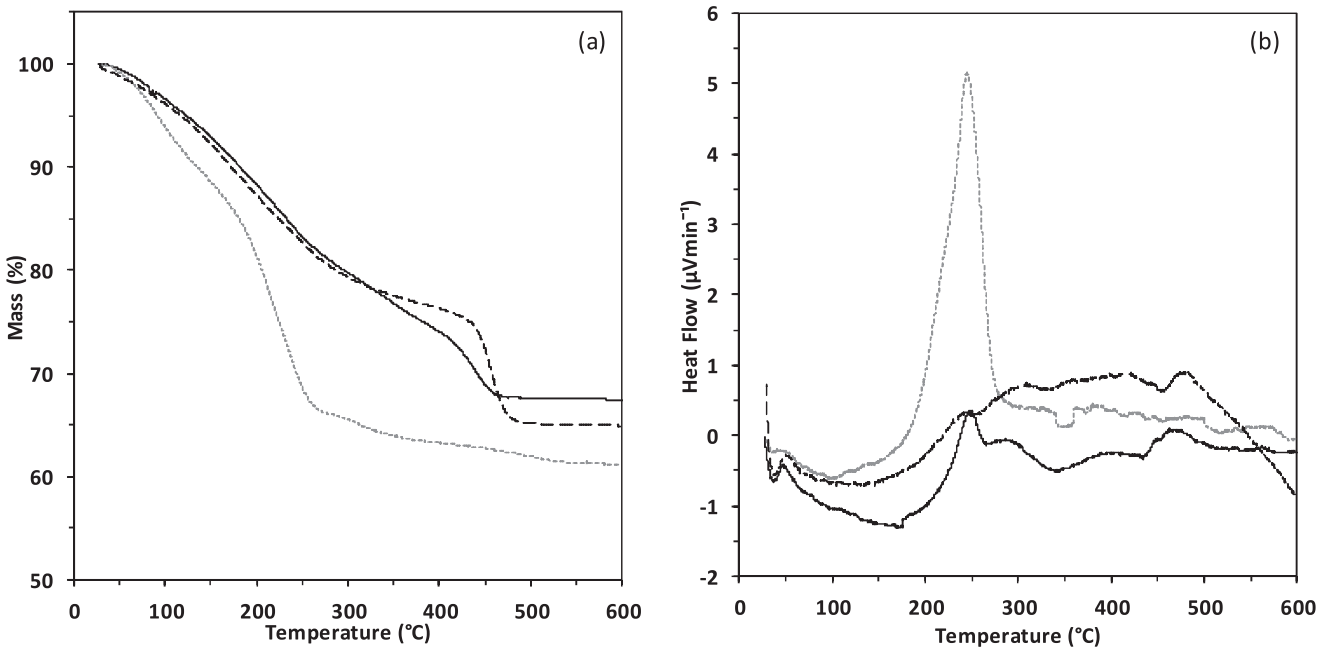

Fig. 3. TGA (a) and DTA (b) analysis of SAS prepared zincian georgeite precursors prepared with and without various Al^{3+} precursors. Analysis performed at a ramp rate of 5 °C min^{-1}in a flow of synthetic air (50 ml min^{-1}). Key:- Binary zincian georgeite (dashed line), Cu/Zn/Al-$C_3H_5O_3$ (grey dotted line) and Cu/Zn/AlO(OH) (solid line).

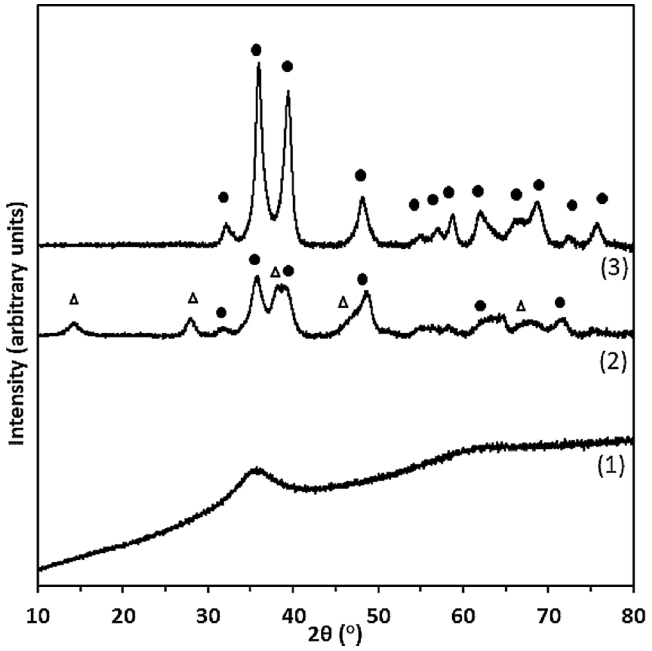

Fig. 4. XRD patterns of calcined SAS zincian georgeite prepared with and without with various Al^{3+} precursors: (1) binary zincian georgeite, (2) CuO/ZnO/AlO(OH) (3) CuO/ZnO/Al-$C_3H_5O_3$ Key:- ● CuO reflections, Δ AlO(OH) reflections.

still an accurate descriptor for methanol synthesis activity and to a lesser extent LTS activity [31].

The Cu surface areas (after reduction at 225 °C) of the two Al containing catalysts and the reference catalysts derived from zincian georgeite are also given in Table 1. The highest reported value was observed for the Cu/ZnO/AlO(OH)catalyst (54 m^2 $g_{Cu}{}^{-1}$), which was greater than that of the lactate derived catalyst (18 m^2 $g_{Cu}{}^{-1}$) and the standard zincian georgeite binary catalyst (47 m^2 $g_{Cu}{}^{-1}$). It is interesting to note that TGA and XRD characterisation of the calcined catalysts and TGA data suggests that the standard binary Cu/Zn catalyst would have the highest Cu dispersion and not Cu/ZnO/AlO(OH), an apparent discrepancy that has a couple of possible explanations. Firstly, the reduction of CuO to metallic Cu is exothermic ($\Delta H = -80.8$ kJ mol^{-1}) and it can be anticipated that a certain degree of Cu sintering will occur during reduction [2]. Specifically, the high concentration of Cu species in these and conventional industrial methanol syntheasis catalysts makes local heat spots during reduction an issue and important factor to consider for catalyst preparation and activation. Potentially the addition of AlO(OH)might physically inhibit sintering of the dispersed Cu and therefore stabilise the higher Cu surface area upon reduction. Alternatively, partial incorporation of Al^{3+} into the ZnO phase could increase the metal support interaction between Cu and ZnO and increase the reducibility of Zn species at the metal support interface [15]. A probable consequence of this effect would be that the N_2O chemisorption value would be inflated by the oxidation of ZnO_x or surface metallic Zn species [30].

The very low Cu surface area value exhibited by Cu/ZnO/Al-$C_3H_5O_3$ confirms the prior observations of large CuO crystallite size and low surface area. Although the relationship between Cu dispersion and catalytic activity, for both methanol synthesis and LTS, has been shown to be a complicated issue [30], there is still a consensus that low Cu surface area catalysts will have poor activity. It was therefore concluded that the Al- lactate derived sample would not be viable catalyst and so was not considered for further catalytic testing. We believe that the methodology of using a soluble Al^{3+} salt could still be a viable option to produce ternary Cu/ZnO/Al_2O_3 catalysts *via* the SAS route However, an extensive screening of different Al^{3+} salts would be required with the key criterion being to choose a ligand that does not decompose as exothermically as the aluminium lactate salt.

Finally, we consider the nanostructure of the Cu/ZnO/AlO(OH) catalyst that will be taken forward to catalytic testing, using STEM analysis. The structure of the 'as-precipitated' and '300 °C calcined' SAS zincian georgeite material has been described in detail elsewhere [23] and will not be repeated here. Representative electron micrographs of the zincian georgeite precursor prepared with the addition of the AlO(OH) sol are shown in Fig. 5. The as-precipitated material (Fig. 5(a)) consists of very characteristic irregularly shaped agglomerates, about

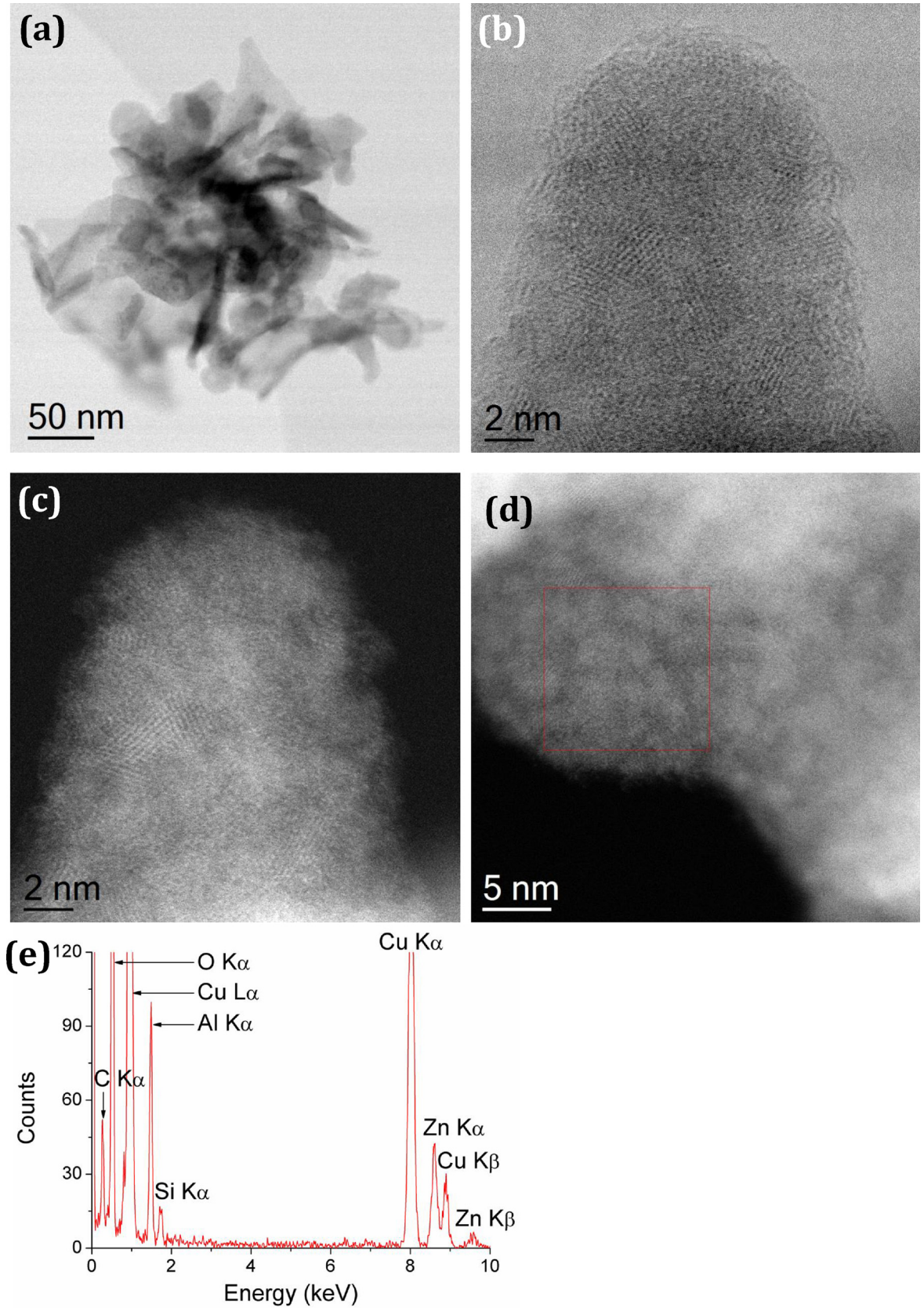

Fig. 5. STEM analysis of the zincian georgeite precursor material prepared with boehmite. (a) HAADF- STEM image showing the general precursor morphology; (b, c) BF-and HAADF-STEM image pair showing isolated sub-2 nm CuO nanocrystallites dispersed in a disordered matrix; (d, e) XEDS spectrum acquired from the highlighted area showing the co-existence of Al, Cu and Zn.

100–200 nm in diameter, of 'amorphous' ~40 nm scale non-facetted particles. Closer inspection by BF- and ADF-STEM, as presented in Fig. 5(b) and (c) shows that these latter particles consist of an amorphous matrix phase, in which are embedded disconnected sub-2 nm crystallites of ordered material exhibiting clear lattice fringes. The amorphous matrix, which is most likely the carbonate and oxyhydroxide component of the material, is by far the majority phase. Analysis of fringe spacings and interplanar angles from this sparse distribution of nanocrystallites (which make up less than 5% by volume of the material) suggest they are most likely CuO. No direct evidence for the existence of discrete AlO(OH) crystallites was found, although a distinct Al signal could be detected in XEDS spectra obtained from most general areas of the sample (*e.g.*, see Fig. 5(d) and (e)). Given XRD has shown crystalline AlO(OH) is present, we conclude that poorly dispersed AlO(OH) is present (to an extent that is difficult to observe at high magnification) in addition to a well distributed Al component within the zincian georgeite matrix. It is interesting to note that Behrens reported that only a small fraction of Al^{3+} was incorporated into traditional zincian malachite type precursors in the co-precipitation methodology [3]. With the exception of the presence of Al, the morphology and nanostructure of this material looks very reminiscent of the precursor zincian georgeite phase described in Ref. [23].

Representative electron micrographs of this same Al containing material after 2 h calcination at 300 °C are shown in Fig. 6. The general morphology of the agglomerates remains the same (Fig. 6(a)) and its high surface area is clearly retained. However, higher magnification STEM imaging (Fig. 6(b) and (c)) reveals that some of the disordered matrix material originally present in the precursor state has now crystallized. However, it should also be noted that a larger volume of disordered matrix remains in comparison to the counterpart 300 °C calcined zincian georgeite material (also described in Ref. [23]). The additional crystallized material is entirely in a nanocrystalline form, with a mean grain diameter of 3–4 nm. Analysis of the fringe spacings and interplanar angles from individual grains suggests the crystalline material is an intimate mixture of zinc and copper oxides.

Methanol synthesis reaction data, normalised to the mass of Cu present, is shown in Fig. 7 for the regular zincian georgeite derived catalyst, the ternary sample prepared with AlO(OH) and an industrial standard catalyst (wt% composition was $CuO/ZnO/Al_2O_3$ = 60;30;10) [32]. Both the Cu/ZnO/AlO(OH) catalyst and the analogous binary zincian georgeite derived catalyst had high initial activity compared to the industrial standard. This high level of activity has been attributed to the high Cu dispersion coupled with a strong interaction with highly disordered ZnO. The higher intrinsic activity of these georgeite derived

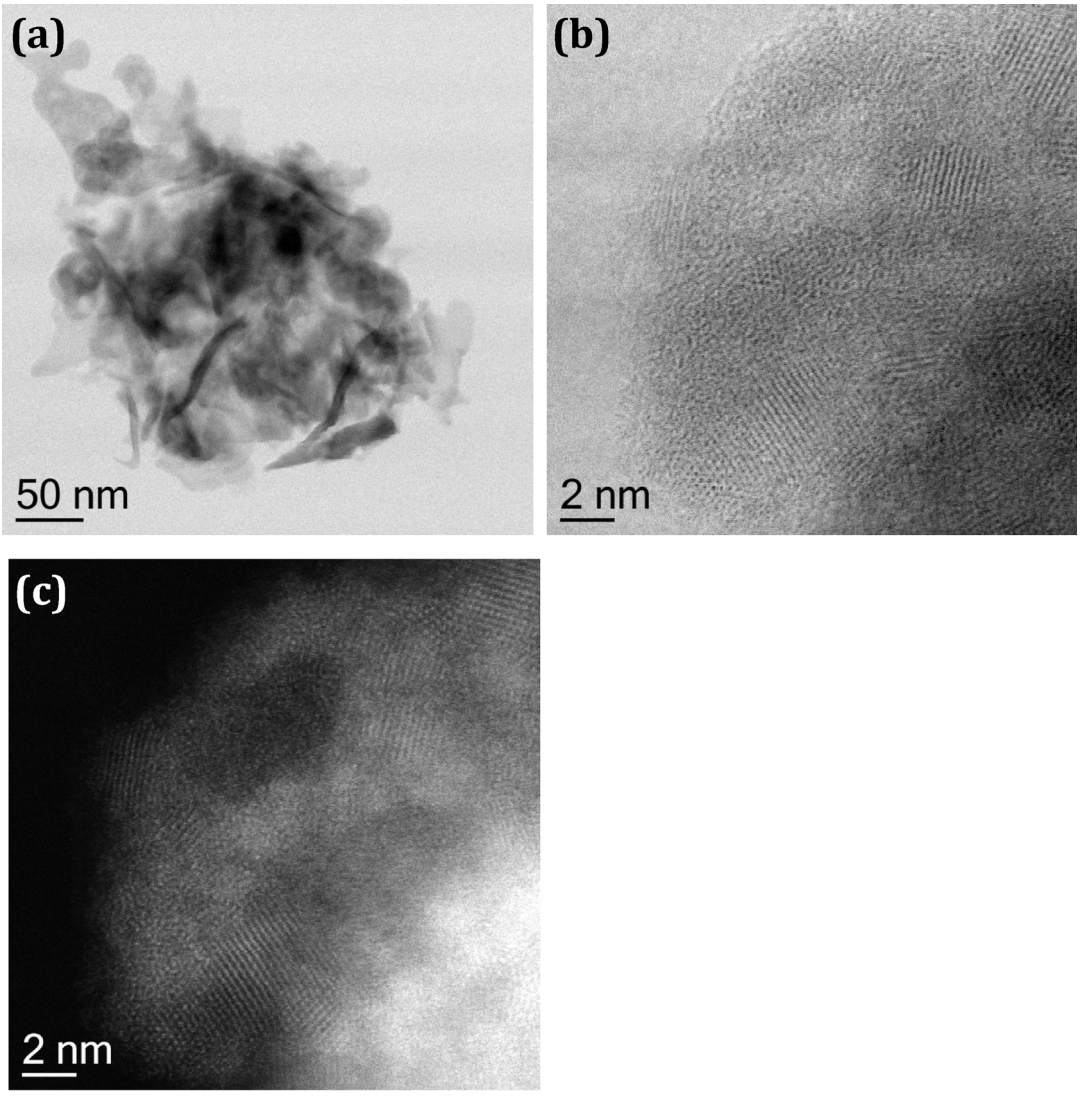

Fig. 6. STEM analysis of the Cu/Zn/Al-AlO(OH) material calcined at 300 °C for 2 h. (a) HAADF-STEM image showing the general catalyst morphology; (b, c) BF-and HAADF-STEM image pair revealing that some of the disordered matrix material originally present in the precursor phase has been converted to 3–4 nm CuO and ZnO nanocrystallites.

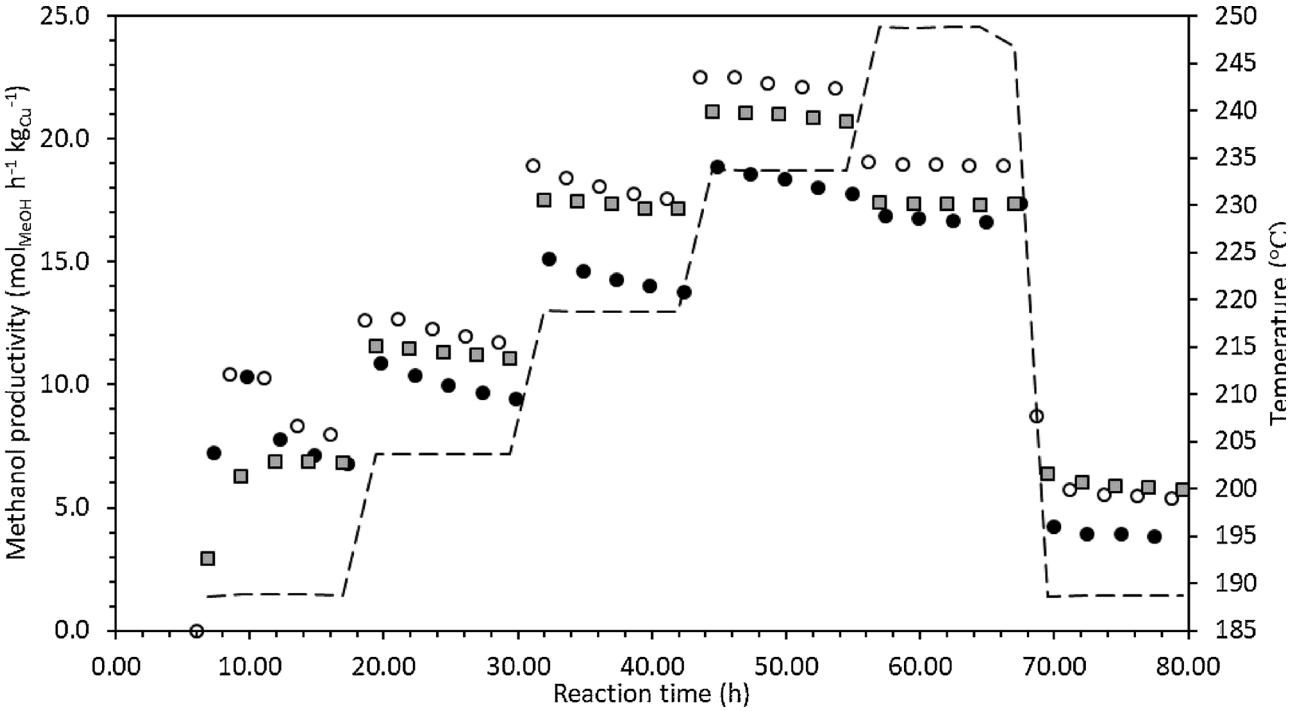

Fig. 7. Time-on-line catalyst testing for the methanol synthesis reaction:.
Reaction temperature was increased 15 °C every 18 h between 190–235 °C.
Reaction conditions for methanol synthesis: 195 °C, 25 bar, gas composition CO:CO_2:H_2:N_2 = 6:9.2:67:17.8, MHSV = 7200 L kg^{-1} h^{-1}. All selectivities to methanol were > 99.96%.
Key:- ● binary zincian georgeite; total mass of Cu in reactor = 0.214 g.
■ Standard commercial Cu/ZnO/Al_2O_3 methanol synthesis catalyst; total mass of Cu in reactor = 0.187 g.
○ Cu/ZnO/AlO(OH):mass of Cu in reactor = 0.212 g.

catalysts is further evident when the productivity was normalised to Cu surface area; with the binary catalyst having a productivity of 8.2 mol_{CH3OH} $m_{Cu}^{2\,-1}$ h^{-1}, the ternary Cu/ZnO/AlO(OH) catalyst 8.6 mol_{CH3OH} $m_{Cu}^{2\,-1}$ h^{-1} and the industrial standard 5.8 mol_{CH3OH} $m_{Cu}^{2\,-1}$ h^{-1}. Unfortunately, in common with the zincian georgeite catalyst, the ternary Cu/ZnO/AlO(OH) catalyst experienced a degree of deactivation over the first 18 h time-on-line. After this time interval, the reaction temperature was increased every 18 h to a maximum of 250 °C, during which the binary catalyst continued to deactivate significantly, in relation to the Cu/ZnO/Al_2O_3 industrial standard. However, the extent of deactivation was substantially reduced for the zincian georgeite sample prepared with the AlO(OH) addition, although some deactivation was still observed above 220 °C. After cycling the temperature to 250 °C temperature was cooled to that used at the start of the testing run (190 °C). Comparison of methanol productivity before and after accelerated ageing shows that the addition of AlO(OH) was beneficial to stability but not to the extent that prolonged productivity was better than the Cu/ZnO/Al_2O_3 industrial standard. While the inclusion of Al^{3+} improved the stability of the zincian georgeite derived catalyst, we consider that a still more significant interaction between Al^{3+} and the Cu/ZnO component is required, which might be achievable from a precipitation based method if a more suitable soluble Al^{3+} precursor can be identified.

In the methanol synthesis reaction, catalyst deactivation is attributed to the sintering of both Cu and ZnO crystallites. *in situ* XRD and neutron diffraction has previously shown that in addition to the expected effect of Cu sintering, ZnO crystallite growth is also strongly correlated with catalyst deactivation [33,34]. In addition, the presence of water in the reaction product stream (seen by in-line FT-IR analysis in the current study for all catalysts) from CO_2 hydrogenation to form methanol and water has been shown to promote ZnO crystallisation [34]. The incorporation of Al^{3+} species potentially enhances the stability of small poorly crystalline ZnO under methanol synthesis conditions.

Catalytic testing results for the LTS reaction for the zincian georgiete, Cu/ZnO/AlO(OH), and a standard industrial LTS catalyst, are shown in Fig. 8. In common with previous studies, the remarkable stability of the zincian georgeite binary catalyst relative to the industrial LTS catalyst was noted once again [23,29]. Interestingly the activity of the Cu/ZnO/AlO(OH) zincian georgeite derived catalyst was even higher and had a similar and if not better stability than the derived binary zincian georgeite catalyst, with almost no deactivation over 130 h time-on-line. The excellent stability of both SAS zincian georgeite-type catalysts can be explained by the low Na^+ content in the samples, which has been shown to be a significant poison, as well as the desirable precursor microstructure of ultra-small CuO crystallites embedded within a disordered ZnO matrix. While the addition of Al^{3+} did impart some marginal improvements to overall catalyst activity and stability, the clear conclusion ion is that the nature of the Cu/Zn precursor in this instance appears to be more influential than the actual addition of Al^{3+} species.

4. Conclusions

The incorporation of Al^{3+} containing species into zincian georgeite derived catalysts has been achieved using two different Al^{3+} precursors; one a soluble aluminium (III) lactate and the other a suspended sol of boehmite (AlO(OH)). Both were added to the conventional 2:1 Cu/Zn acetate solutions and sprayed into $scCO_2$. It was demonstrated that both precursors could be successfully precipitated along with zincian georgeite. Ultimately the use of aluminium(III) lactate was not viable, as the salt was retained upon SAS precipitation and decomposed exothermally during calcination, yielding a very low Cu surface area relative to the standard zincian georgeite material. While the use of

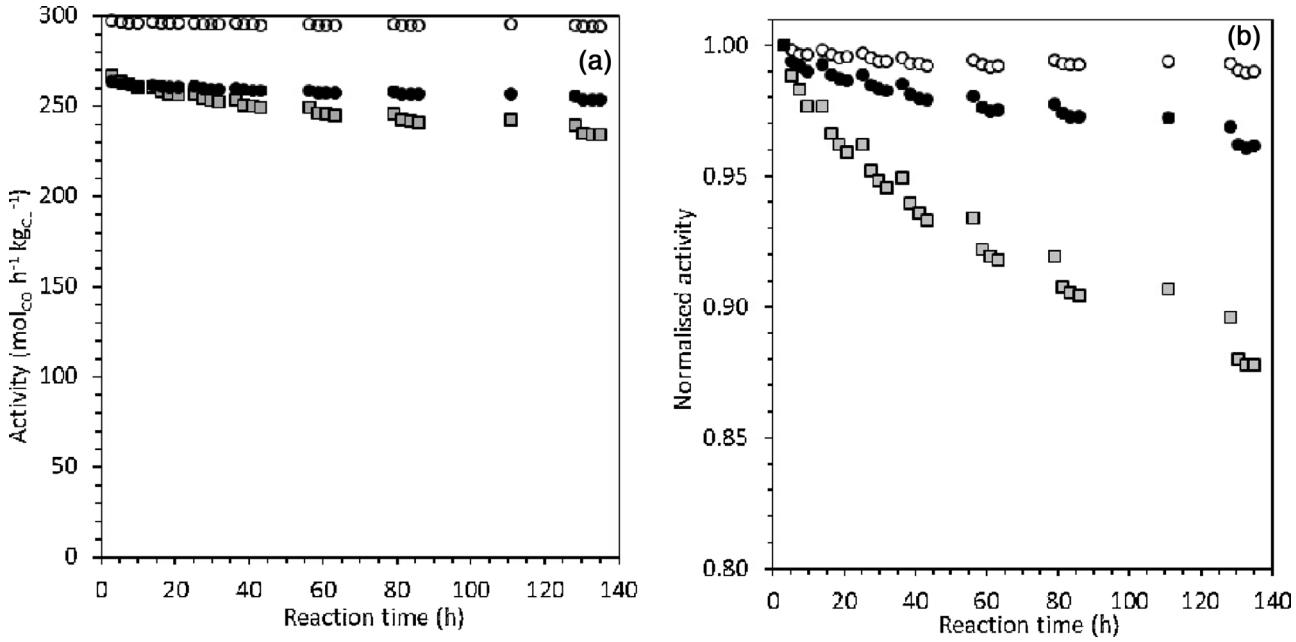

Fig. 8. Time-on-line (Cu mass normalised) low temperature water gas shift reaction results; (a) Activity normalised to Cu mass (b) Normalised activity shown to highlight deactivation profiles.
Reaction conditions for low temperature water gas shift: 220 °C, 27.5 bar, gas composition H_2O:CO:CO_2:H_2:N_2 = 50:2:8:27.5:12.5, MHSV = 75,000 L kg^{-1} h^{-1}.
Key:-● binary zincian georgeite: total mass of Cu in reactor = 0.214 g.
■ Standard commercial Cu/ZnO/Al_2O_3 LTS catalyst, total mass of Cu in reactor = 0.200 g.
○ CuO/ZnO/AlO(OH); total mass of Cu in reactor = 0.212 g.

soluble aluminium salt was shown not to be successful when using aluminium lactate, other salts that decompose less exothermically may be viable alternatives. By way of comparison, the incorporation of AlO(OH) slightly improved Cu dispersion by imparting increased stability, despite having a marginally negative effect on the extent of Cu-Zn mixing in the original SAS precipitate and resulting calcined materials. The addition of Al^{3+} in the form of boehmite notably improved catalyst stability for the methanol synthesis reaction and to a lesser extent in the LTS reaction.

Acknowledgments

We would like to thank the EPSRC and UK Catalysis Hub for funding (grants EP/K014714/1, EP/K014714/1, EP/K014668/1, EP/K014706/1, EP/H000925/1, EP/I019693/1 and EPSRC Grant EP/L027240/1). CJK gratefully acknowledges funding from the National Science Foundation Major Research Instrumentation program (GR# MRI/DMR-1040229). In addition, we would like to thank Johnson Matthey for their support in the research.

References

[1] G.C. Chinchen, P.J. Denny, J.R. Jennings, M.S. Spencer, K.C. Waugh, Appl. Catal. 36 (1988) 1–65.
[2] C. Rhodes, G.J. Hutchings, A.M. Ward, Catal. Today 23 (1995) 43–58.
[3] M. Behrens, Angew. Chem. Int. Ed. 53 (2014) 12022–12024.
[4] E. Kunkes, M. Behrens, Methanol Chemistry, Walter de Gruyter GmbH, 2013, pp. 413–441.
[5] R. Burch, Phys. Chem. Chem. Phys. 8 (2006) 5483–5500.
[6] G.C. Chinchen, K.C. Waugh, D.A. Whan, Appl. Catal. 25 (1986) 101–107.
[7] M.S. Spencer, Top. Catal. B (1999) 259–266.
[8] S. Kattel, P.J. Ramírez, J.G. Chen, J.A. Rodriguez, P. Liu, Science 355 (2017) 1296–1299.
[9] M. Behrens, F. Studt, I. Kasatkin, S. Kühl, M. Hävecker, F. Abild-Pedersen, S. Zander, F. Girgsdies, P. Kurr, B.-L. Kniep, M. Tovar, R.W. Fischer, J.K. Nørskov, R. Schlögl, Science 336 (2012) 893–897.
[10] G. Dutta, A.A. Sokol, C.R.A. Catlow, T.W. Keal, P. Sherwood, Chem. Phys. Chem. 13 (2012) 3453–3456.
[11] S. Kuld, M. Thorhauge, H. Falsig, C.F. Elkjær, S. Helveg, I. Chorkendorff, J. Sehested, Science 352 (2016) 969–974.
[12] T. Fujitani, J. Nakamura, Catal. Lett. 56 (1998) 119–124.
[13] B.S. Clausen, H. Topsøe, Catal. Today 9 (1991) 189–196.
[14] P.L. Hansen, J.B. Wagner, S. Helveg, J.R. Rostrup-Nielsen, B.S. Clausen, H. Topsøe, Science 295 (2002) 2053–2055.
[15] M. Behrens, S. Zander, P. Kurr, N. Jacobsen, J. Senker, G. Koch, T. Ressler, R.W. Fischer, R. Schloegl, J. Am. Chem. Soc. 135 (2013) 6061–6068.
[16] M.S. Spencer, M.V. Twigg, Annu. Rev. Mater. Res. 35 (2005) 427–464.
[17] J.S. Campbell, Ind. Eng. Chem. Process Des. Dev. 9 (1970) 588–595.
[18] M. Behrens, J. Catal. 267 (2009) 24–29.
[19] M. Behrens, F. Girgsdies, Zeitschrift Fur Anorganische Und Allgemeine Chemie 636 (2010) 919–927.
[20] B. Bems, M. Schur, A. Dassenoy, H. Junkes, D. Herein, R. Schlogl, Chem.– Eur. J. 9 (2003) 2039–2052.
[21] E. Reverchon, J. Supercrit. Fluids 15 (1999) 1–21.
[22] P.J. Bridge, J. Just, M.H. Hey, Miner. Mag. 43 (1979) 97–98.
[23] S.A. Kondrat, P.J. Smith, P.P. Wells, P.A. Chater, J.H. Carter, D.J. Morgan, E.M. Fiordaliso, J.B. Wagner, T.E. Davies, L. Lu, J.K. Bartley, S.H. Taylor, M.S. Spencer, C.J. Kiely, G.J. Kelly, C.W. Park, M.J. Rosseinsky, G.J. Hutchings, Nature 531 (2016) 83–87.
[24] R.P. Marin, S.A. Kondrat, J.R. Gallagher, D.I. Enache, P. Smith, P. Boldrin, T.E. Davies, J.K. Bartley, G.B. Combes, P.B. Williams, S.H. Taylor, J.B. Claridge, M.J. Rosseinsky, G.J. Hutchings, ACS Catal. 3 (2013) 764–772.
[25] M. Behrens, F. Girgsdies, A. Trunschke, R. Schlögl, Eur. J. Inorg. Chem. (2009) 1347–1357.
[26] A.M. Pollard, M.S. Spencer, R.G. Thomas, P.A. Williams, J. Holt, J.R. Jennings, Appl. Catal. A 85 (1992) 1–11.
[27] A.M. Pollard, R.G. Thomas, P.A. Williams, J. Just, P.J. Bridge, Miner. Mag. 55 (1991) 163–166.
[28] M. Schur, B. Bems, A. Dassenoy, I. Kassatkine, J. Urban, H. Wilmes, O. Hinrichsen, M. Muhler, R. Schlögl, Angew. Chem. Int. Ed. 42 (2003) 3815–3817.
[29] P.J. Smith, S.A. Kondrat, J.H. Carter, P.A. Chater, J.K. Bartley, S.H. Taylor, M.S. Spencer, G.J. Hutchings, ChemCatChem 9 (2017) 1621–1631.
[30] M.B. Fichtl, J. Schumann, I. Kasatkin, N. Jacobsen, M. Behrens, R. Schlögl, M. Muhler, O. Hinrichsen, Angew. Chem. – Int. Ed. 53 (2014) 7043–7047.
[31] R.A. Hadden, P.J. Lambert, C. Ranson, Appl. Catal. A: Gen. 122 (1995) L1–L4.
[32] G.D. Short, G.C. Chinchen, J.G. Williamson, Synthesis of methanol: finely divided oxides of zinc, aluminium, magnesium; with metallic copper. US patent, 4, (1988), 788, 175.
[33] T. Lunkenbein, F. Girgsdies, T. Kandemir, N. Thomas, M. Behrens, R. Schlögl, Angew. Chem. Int. Ed. 128 (2016) 12900–12904.
[34] S.A. Kondrat, P.J. Smith, J.H. Carter, J.S. Hayward, G.J. Pudge, G. Shaw, M.S. Spencer, J.K. Bartley, S.H. Taylor, G.J. Hutchings, Faraday Discuss. 197 (2017) 287–307.